Numerical Analysis of Slow-Wave Instabilities in an X-Band Sinusoidally Corrugated Waveguide with Coaxial Slow-Wave Structure

Shingo ABE, Kazuo OGURA, Kosuke OTUBO and Hiroki KIMURA

Graduate School of Science and Technology, Niigata University, Niigata 950-2181, Japan

(Received 9 December 2009 / Accepted 16 March 2010)

The dispersion characteristics and slow-wave instabilities of a sinusoidally corrugated waveguide with coaxial slow-wave structure (SWS) are analyzed. In SWS, a central cylindrical conductor is surrounded by an outer cylindrical conductor. Sinusoidal corrugation is formed on either conductor or both conductors. The corrugation parameters are those used for an X-band SWS. The relative phase between the sinusoidal corrugations on the inner and outer conductors affects the dispersion characteristics. Instabilities due to beam interactions with the slow -waves are examined by considering three-dimensional beam perturbations. The slow cyclotron instability occurs in addition to the Cherenkov instability, since transverse as well as longitudinal perturbations are included.

Keywords: coaxial slow-wave structure, backward wave oscillator, surface wave, slow cyclotron instability, Cherenkov instability

DOI: 10.1585/pfr.5.S2091

1. Introduction

A backward wave oscillator (BWO) is a high-power microwave source that can be driven by an axially injected electron beam. In such slow-wave devices, slow-wave structures (SWSs) are used to reduce the phase velocity of the electromagnetic wave to close to the beam velocity. An SWS is typically a hollow circular waveguide with a periodically corrugated wall. Electron beams are injected into the SWS and interact with the slow-waves. Theoretical studies of slow-wave interactions in such configurations have been reported [1–3]. Another type of SWS is a coaxial SWS [4–6] in which a central conductor is installed on the axis. It has been noted that the coaxial types have potentially attractive features such as the ability to maintain a wide frequency based on the transverse electromagnetic (TEM) mode, increasing the operation frequency and improving the conversion efficiency.

A transverse electric (TE) and transverse magnetic (TM) waveguide modes are available. The TE mode has no axial electric field element, and the TM mode has no axial magnetic field element. When waveguide modes are influenced by magnetized beams, the result is a hybrid mode in which the TE and TM modes coexist [7]. In coaxial waveguides, the TEM mode occurs as a fundamental mode. The TEM mode has neither an axial electric field nor an axial magnetic field element, but it has a radial electric field element. However, in coaxial SWSs with corrugations, the TEM mode has an electric field element in the axial direction and is called the “quasi-TEM” mode [4]. In this case, beam interactions via the axial electric field of the quasi-TEM mode become possible.

In coaxial SWSs, a central cylindrical conductor is surrounded by an outer cylindrical conductor. Sinusoidal corrugations are formed on either conductor or both conductors. In the latter, the phase lag of the inside corrugation relative to the outside one can be changed. The relative phase between the sinusoidal corrugations of the inner and outer conductors affects the dispersion characteristics [5].

In this study, we develop a numerical code for a sinusoidally corrugated waveguide with coaxial SWS and analyze the dispersion characteristics and slow-wave instabilities of coaxial SWSs. This paper is organized as follows. In Section 2, we describe a numerical model for analyzing coaxial SWSs. In Section 3, we examine the dispersion characteristics of an X-band coaxial SWS and the slow-wave instabilities of a coaxial SWS driven by an annular beam. In Section 4, we resent our conclusions.

2. Numerical Methods

To analyze electromagnetic waves in a coaxial SWS, we consider two types of coaxial SWS with sinusoidal corrugation, as shown in Fig. 1. In Type 1, the outer waveguide wall radius $R_w(z)$ varies along the axial direction z as $R_{\text{out}} + h\cos(k_0 z)$. Here, R_{out}, h, z_0, and $k_0 = 2\pi/z_0$ are the average outer radius, corrugation amplitude pitch length and corrugation wave number, respectively. The inner radius R_{in} is constant in this case. In Type 2, in addition to the outer corrugation $R_{\text{w}}(z)$, the radius of the inner conductor varies along the axial direction z as $R_{\text{in}} + h\cos(k_0 z)$. Here, R_{in} is the average inner radius. A guiding magnetic field B_0 is applied uniformly in the axial direction. An annular

author's e-mail: teogura@eng.niigata-u.ac.jp

electron beam of radius R_b propagates in the axial direction between the outer and inner conductors.

The temporal and spatial phase factor of all perturbed quantities is assumed to be $\exp[i(k_z z + m\theta - \omega t)]$. Here, m is the azimuthal mode number and k_z is the axial wave number. With this assumption, the dispersion relation can be derived self-consistently considering three-dimensional beam perturbations in accordance with the method in Refs. [1, 8]. For the beam, relativistic effects are considered.

In a system with a magnetized beam such as that shown in Fig. 1, the electromagnetic modes are hybrids of the TM and TE modes because of the perturbed motion perpendicular to the magnetic field. The letters EH and HE are used, to designate the hybrid modes. In this paper,

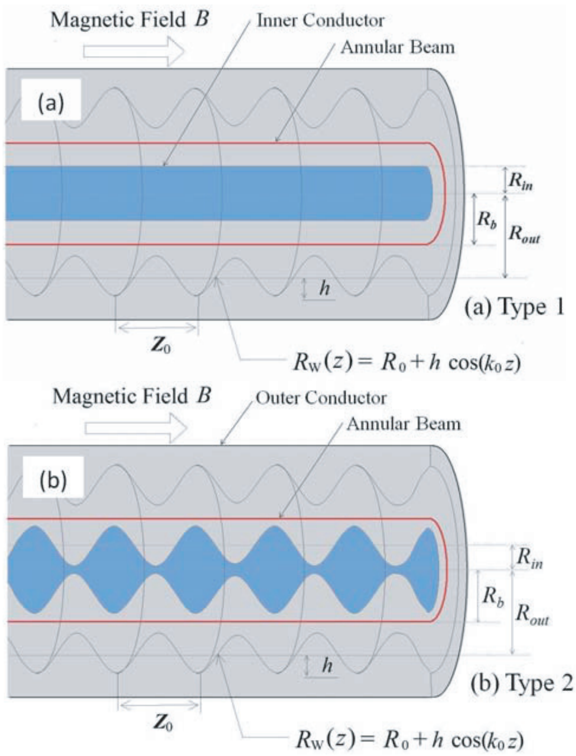

Fig. 1 Model for analysis: (a) Type 1 and (b) Type 2 coaxial SWS.

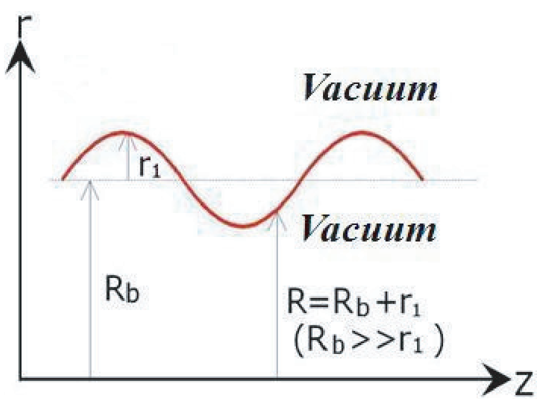

Fig. 2 Beam surface of infinitesimally thin annular beam.

TM is dominant in the EH mode, and TE is dominant in the HE mode [7].

In our model, we assume an infinitesimally thin annular beam. The sheet electron beam's surface is modulated as the beam propagates as shown in Fig. 2. Because displacement in the vertical direction cannot be treated as a surface charge as in Refs. [1, 7], the perturbation of the sheet beam is treated following the method of Ref. [8]. Boundary conditions at the corrugations are formulated using the methods in Ref. [1].

3. Numerical Results

First, we analyze a coaxial waveguide without an electron beam. Figure 3 shows the dispersion curves of a Type 1 coaxial SWS without a beam for two values of corrugation amplitude, $h = 0.445$ cm and 0.1 cm. For the other geometrical parameters, we choose the X-band values of Refs. [4–6]: $R_{out} = 1.445$ cm, $R_{in} = 0.5$ cm, and $z_0 = 1.67$ cm. According to Floquet's theorem, known as Bloch's theorem in solid-state physics, the dispersion curves of spatially periodic SWSs are periodic in wave number space (k_z-space). For a spatially periodic SWS with a period of z_0, the corresponding period in k_z-space is $k_0 = 2\pi/z_0$. Since a one-period drawing has all the information on the dispersion characteristics, the dispersion curves are depicted over one period of $0 < k_z < k_0$. Other regions in k_z-space are reduced to the region of $0 < k_z < k_0$.

In Fig. 3, the black and red curves are the dispersion curves for $h = 0.445$ and 0.1 cm, respectively. The blue curves are those of the TM_{01} mode in the limit of $h \to 0$, which corresponds to a straight cylindrical coaxial waveguide. It can be said that the higher-order mode represented by the red line is composed of the TM and quasi-TEM modes. This higher-frequency mode is called the A mode in Refs. [4, 5] and has a frequency close to the cutoff frequency of the TM mode of a straight cylindrical waveguide

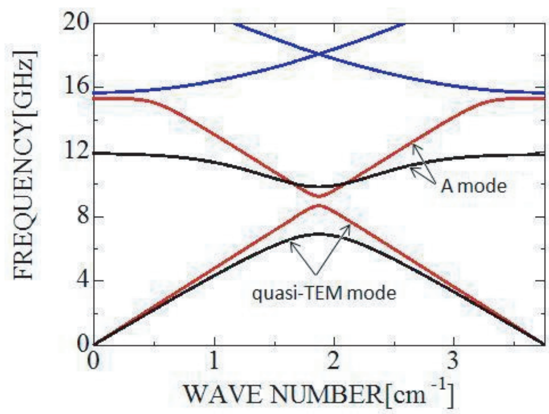

Fig. 3 Dispersion curves of Type 1 coaxial SWS without an electron beam for corrugation amplitude $h = 0.445$ cm (black curve) and 0.1 cm (red curve), $R_{out} = 1.445$ cm, $R_{in} = 0.5$ cm and $z_0 = 1.67$ cm.

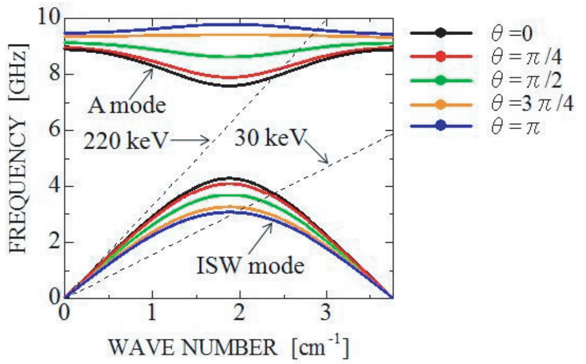

Fig. 4 Dispersion curves of Type 2 coaxial SWS without an electron beam. Relative phase θ is changed from zero to π with a step of $\pi/4$. Dotted lines show the beam space charge mode lines of 220 keV and 30 keV, with infinitesimal current. The former energy corresponds to Fig. 5 and the latter to Fig. 7.

at $k_z = 0$. The A mode is influenced by the quasi-TEM mode, and the frequency decreases as k_z approaches the π point, at which $k_z z_0 = \pi$, that is, $k_z = k_0/2 = 1.88\,\mathrm{cm}^{-1}$. By increasing h, the frequency of the higher-order A mode is decreased, as shown by the black curve for $h = 0.445$ cm.

Figure 4 shows the dispersion curves of a Type 2 coaxial SWS without a beam, in which the relative phase θ between the inner and outer sinusoidal corrugations is changed with a step of $\pi/4$. The quasi-TEM mode becomes a surface wave mode of the inner corrugation and is referred to as the inner surface wave (ISW) mode. The upper cutoff frequency of the ISW mode decreases as θ increases from zero to π. In contrast, the frequency of A the mode increases as θ increases from zero to π. The curve of the A mode is fairly flat. It is depressed near the π point with $\theta = 0$ and rises with increasing θ. The group velocity at the crossing point of the A mode and the light line is positive at $\theta = 0$. This group velocity becomes negative as θ approaches π.

Next, we analyze the slow-wave instability of a coaxial SWS with sinusoidal corrugation driven by an annular beam. Figure 5 shows the dispersion curves with a beam energy of 220 keV, current of 100 A, beam radius R_b = 0.8 cm, magnetic field B = 0.3 T, and relative phase θ = π. The SWS parameters are the same as in Fig. 4.

The waveguide mode becomes a hybrid of the TE and TM modes because of the influence of the magnetized beams, even in the axisymmetric case. For example, the TM_{01} mode becomes the EH_{01} mode because of the existence of the magnetized electron beam [7]. Figure 5 shows the axisymmetric case, and the A mode corresponds to the EH_{01} mode in a hollow waveguide. With the magnetized beam, there are space charge modes, the slow cyclotron mode, and the fast cyclotron mode. The slow space charge and slow cyclotron modes couple to the A mode, leading to the Cherenkov and slow cyclotron instabilities, respectively. Note that the periodic dispersion curves are depicted

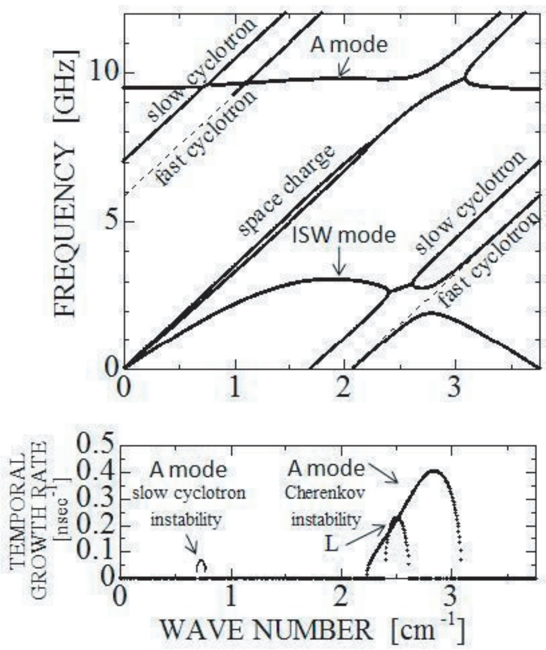

Fig. 5 Dispersion curves of Type 2 coaxial SWS with a beam energy of 220 keV, current of 100 A, beam radius R_b = 0.8 cm, magnetic field B = 0.3 T, and relative phase θ = π. Instability L is the slow cyclotron instability of the ISW mode.

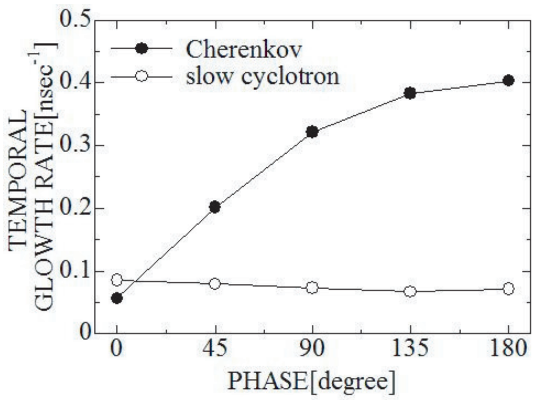

Fig. 6 Cherenkov and slow cyclotron instabilities of the A mode versus the relative phase between the inner and outer conductors.

in one period region of $0 < k_z < k_0$. Hence, the slow cyclotron instability in the region from k_0 to $3k_0/2$ is seen in the region from 0 to $k_0/2$. The temporal growth rates of these instabilities are shown in the lower frame of Fig. 5. Instability L is the slow cyclotron instability of the ISW mode. The Cherenkov instability of the ISW mode does not exist, since the beam energy is too high for the space charge mode to interact with the ISW mode. In Fig. 6, the peak values of the instability of the A mode are plotted as a function of θ. The Cherenkov instability strengthens as θ increases, whereas the slow cyclotron instability decreases slightly with increasing θ.

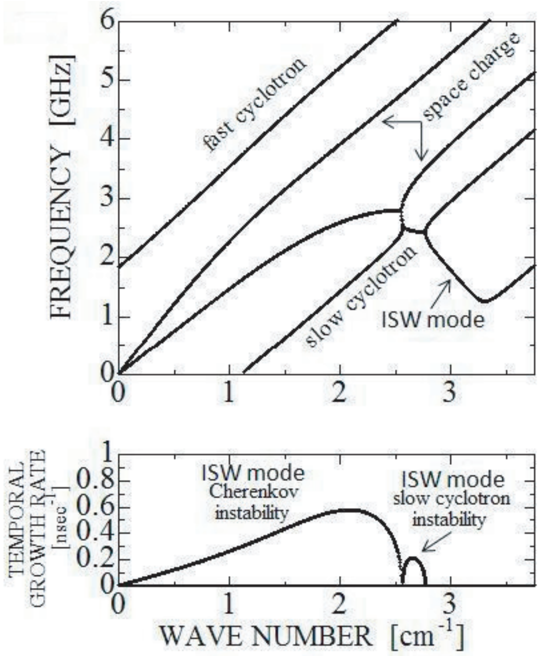

Fig. 7 Dispersion curves of Type 2 coaxial SWS. Beam energy is 30 keV. Other parameters are the same as in Fig. 5.

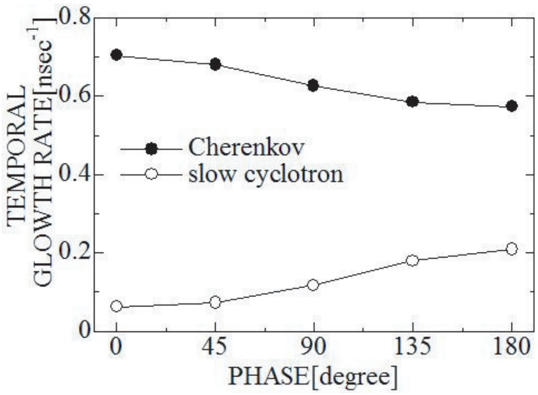

Fig. 8 Cherenkov and slow cyclotron instabilities of the ISW mode versus the relative phase between the inner and outer conductors.

The Cherenkov instability of the ISW mode will appear if the beam energy decreases. In Fig. 7, dispersion curves of the ISW mode are calculated at a beam energy of 30 keV. The other parameters are the same as in Fig. 5. In Fig. 7, both the Cherenkov instability and the slow cyclotron instability of the ISW mode appear. Figure 8 shows the dependence of the ISW instabilities on θ. As θ increases, the Cherenkov instability decreases and the slow cyclotron instability increases. This dependence is in contrast to that of the A mode in Fig. 6.

4. Conclusion

We developed a numerical code for a sinusoidally corrugated waveguide with a coaxial SWS driven by a infinitesimally thin annular beam considering three-dimensional beam perturbations. Because of the inner conductor, the quasi-TEM mode is the fundamental mode, the next higher-frequency mode consists of the TEM and TM modes and is designated as the A mode. The A modes are greatly influenced by the phase lag of the inner corrugation relative to the outer one. The Cherenkov instability of the A mode increases as the phase lag shifts from zero to π. In contrast, the Cherenkov instability of the ISW mode decreases as the phase lag increases from zero to π.

Acknowledgments

This study was partially supported by a Grant-in-Aid for Scientific Research from the Ministry of Education, Science, Sports and Culture of Japan, and by the NIFS Collaboration Research Program.

[1] K. Ogura *et al.*, Jpn. J. Appl. Phys. **42**, 7095 (2003).
[2] H. Yamazaki *et al.*, IEEJ Trans. FM. **124**, 477 (2004).
[3] H. Yamazaki *et al.*, IEEJ Trans. FM. **125**, 739 (2005).
[4] X. Zheng *et al.*, J. Phys. Soc. Jpn. **64**, 1042 (1995).
[5] X. Renzhen *et al.*, IEEE Trans. Plasma Sci. **35**, 1456 (2007)
[6] G. Liu *et al.*, J. Appl. Phys. **103**, 093303 (2008).
[7] O. Watanabe *et al.*, Phys. Rev. E **63**, 056503 (2001).
[8] K. Ogura *et al.*, J. Plasma Phys. **72**, 905 (2006).